Available online at www.sciencedirect.com
SCIENCE DIRECT®
Journal of Solid State Chemistry 178 (2005) 2109–2116
JOURNAL OF SOLID STATE CHEMISTRY
www.elsevier.com/locate/jssc

Structural and conductivity study of a new protonic conductor $Cs_{0.86}(NH_4)_{1.14}SO_4 \cdot Te(OH)_6$

M. Dammak[a,c,*], L. Ktari[a], A. Cousson[b], T. Mhiri[a]

[a] *Laboratoire de l'Etat Solide (LES), Faculté des Sciences de Sfax, 3018 Sfax, Tunisie*
[b] *Laboratoire Léon Brouillon, CEA Saclay, 91191 Gif-Sur-Yvette Cedex, France*
[c] *Laboratoire de Chimie Inorganique (LCI), Faculté des Sciences de Sfax, 3018 Sfax, Tunisie*

Received 31 January 2005; received in revised form 22 March 2005; accepted 6 April 2005

Abstract

The crystal structure of $Cs_{0.86}(NH_4)_{1.14}SO_4 \cdot Te(OH)_6$ is determined by X-ray diffraction analysis. The space group is $P2_1/c$ with $a = 13.681(3)$ Å, $b = 6.608(1)$ Å, $c = 11.362(2)$ Å, $\beta = 106.65(3)^\circ$ and $Z = 4$ at 293 K. The structure is refined to $R = 2.9\%$. The distribution of atoms can be described as isolated TeO_6 octahedra and SO_4 tetrahedra. The Cs^+ and NH_4^+ cations, occupying the same positions, are located between these polyhedra. The main feature of this structure is the coexistence of two types of anions in the same crystal related by network hydrogen bonds.

The mixed solid solution cesium ammonium sulphate tellurate exhibits two phase transitions at 470 and 500 K. These transitions, detected by differential scanning calorimetric, are analyzed by dielectric measurements using the impedance and modulus spectroscopy techniques.

Keywords: Structure; Cesium; Tellurate; Conduction; DSC

1. Introduction

The compounds of general formula $M_nAO_4.Te(OH)_6$, where (M = Na, K, NH_4, Rb, Cs, A = S, Se, P and $n = 2, 3$) have attracted much attention for their structural phase transitions and their associated physical properties: ferroelectricity, dielectric relaxation and especially a phase transition into a state characterized by a high protonic conductivity [1–4].

The influence of cationic substitution on crystal symmetry and physical properties has been reported in previous studies for a new mixed solution of rubidium ammonium sulphate tellurate which crystallizes in $P2_1/a$ space group at room temperature and in $P2$ one at high temperature [5,6]. In the other hand, the potassium ammonium sulphate tellurate exhibits $P2_1/a$ space group [7]. In order to examine the effect and influence of cationic substitution on crystalline symmetry and physical properties, we have extended our research to the cesium ammonium sulphate tellurate mixed solution $Cs_{0.86}(NH_4)_{1.14}SO_4 \cdot Te(OH)_6$ (CsNST). At room temperature, CsNST crystals crystallize in the $P2_1/c$ space group.

Based compounds $Cs_2SO_4 \cdot Te(OH)_6$ (CsST) and $(NH_4)_2SO_4 \cdot Te(OH)_6$ (NST) were described in previous works [8–10]. Indeed, CsST crystallizes in $R3$ space group whereas NST belongs to the monoclinic space group Cc. In the present work, we describe the structure of a new CsNST compound and we try to predict its physical properties on the bases of the structure determination.

*Corresponding author. Laboratoire de Chimie Inorganique (LCI), Faculté des Sciences de Sfax, 3018 Sfax, Tunisie. Fax: 216 74274437.
E-mail address: meddammak@yahoo.fr (M. Dammak).

0022-4596/$ - see front matter © 2005 Elsevier Inc. All rights reserved.
doi:10.1016/j.jssc.2005.04.013

2. Experimental details

Single crystals of $Cs_{0.86}(NH_4)_{1.14}SO_4 \cdot Te(OH)_6$ were grown by slow evaporation from a mixture of telluric acid H_6TeO_6 and corresponding sulphates $(NH_4)_2SO_4$ and Cs_2SO_4 in stoichiometric ratio (1/1/1). Schematically the reaction is:

$$H_6TeO_6 + x\ (NH_4)_2SO_4 + (1-x) \rightarrow$$
$$Cs_2SO_4\ Cs_{2-2x}\ (NH_4)_{2x}SO_4 \cdot Te(OH)_6$$

The formula is determined by refinement of the crystal structure and confirmed by chemical analysis. Calorimetric measurements were performed between 300 and 750 K with a DSC SETARAM 92.

The X-ray single crystal was carried out using Kappa-CCD diffractometer with graphite monochromated Mo$K\alpha$ radiation [11]. The unit cell parameters are identified and refined using the Denzo program [12]. The X-ray data are collected using the Collect program [13]. The integrated intensities were corrected for Lorentz and polarization effects [14]. All subsequent computations were carried out using the computer program SHELX [15,16]. The structure was solved by conventional Patterson and difference-Fourier techniques and refined by the full matrix least squares procedure. Hydrogen atoms were located from the electron density difference map.

Dielectric measurements were carried out on pellets with dimensions approximately 13 mm in diameter and 1 mm in thickness. Electrical impedance was measured in the range 100 Hz–13 MHz using a Hewlett-Packard 4192 A LF automatic bridge monitored by an HP Vectra microcomputer.

3. Results and discussion

3.1. Structural study

Fig. 1 shows a projection on the *ac* plane of CsNST structure. In this structure, we note the presence of two different and independent anions in the same crystal.

The structure can be regarded as being built of planes of pure SO_4 tetrahedra altering with planes of pure TeO_6 octahedra, parallel to the (100) and (001) planes. The Cs^+/NH_4^+ cations are situated between these kinds of polyhedra.

The details of data collection, the final atomic positions and U_{eq} parameters for the CsNST compound are given in Tables 1–3 whereas the main interatomic distances and bond angles for TeO_6 octahedra and SO_4 tetrahedra are given in Tables 4 and 5.

The Te atom in CsNST structure, occupies two special positions. In consequence, the structure shows two kinds of octahedra $Te(1)O_6$ and $Te(2)O_6$, with Te–O values between 1.913(3) and 1.917(3) Å. The O–Te–O angles vary from 87.7(1)° to 92.3(1)°. In comparison with the sulphate tellurate studies, the Te–O distances and O–Te–O angles show that the octahedra are regular in the CsNST structure. Indeed, in the $Cs_2SO_4.Te(OH)_6$ compound, the Te–O distances spread from 1.905 to

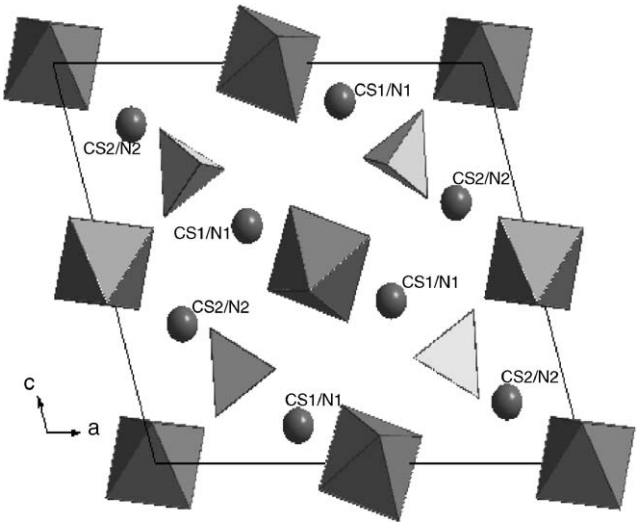

Fig. 1. Projection of $Cs_{0.86}(NH_4)_{1.14}SO_4Te(OH)_6$ crystal structure at 293 K on the *ac* plane.

Table 1
Main Crystallographic data for $Cs_{0.86}(NH_4)_{1.14}SO_4Te(OH)_6$

Formula	$Cs_{0.86}(NH_4)_{1.14}SO_4Te(OH)_6$
Formula weight (g mol^{-1})	460.5
Crystal system	Monoclinic
a (Å)	13.681 (3)
b (Å)	6.608 (1)
c (Å)	11.362 (2)
β (°)	106.65 (3)
V (Å^3)	984.1 (3)
Z	4
Space group	$P2_1/c$
θ min./θ max.(°)	3.11/25.65
T (K)	293 (2)
Diffractometer	Enraf-Nonius Kappa CCD
λ (Mo$K\alpha$)(Å)	0.71073
$-16 \leqslant h \leqslant 15$	
$-8 \leqslant k \leqslant 0$	
$0 \leqslant l \leqslant 13$	
Measured reflections	2018
Independent reflections	1823
Reflections with $I > 4\sigma(I)$	1344
R_{int}	0.042
ρ_{cal} (g cm^{-3})	2.46
μ (cm^{-1})	105.6
min., max., $\Delta\rho$ (e/Å^3)	−0.71, 0.66
Parameters refined	133
R (F)[a]%	2.9
wR (F)[a]%	10.85

[a] R values are defined as $wR_2 = (\sum[w(F_o^2-F_c^2)^2]/[w(F_o^2)^2])^{1/2}$ and $R_1 = \sum||F_o|-|F_c||/\sum|F_o|$.

Table 2
Fractional atomic coordinates and thermal displacement factors for $Cs_{0.86}(NH_4)_{1.14}SO_4Te(OH)_6$

Atoms	X	Y	Z	U_{eq} (Å^3)
Te_1	0.5000	0.0000	0.0000	0.0122 (2)
Te_2	1.0000	1.0000	0.5000	0.0118 (2)
S	0.7509 (7)	0.5086 (1)	0.2647 (1)	0.0135 (4)
Cs_1	0.6454 (2)	0.4975 (3)	−0.0931 (4)	0.029 (1)
N_1	0.6454 (2)	0.4975 (3)	−0.0931 (4)	0.029 (1)
Cs_2	0.8548 (3)	0.4860 (4)	0.6524 (5)	0.023 (1)
N_2	0.8548 (3)	0.4860 (4)	0.6524 (5)	0.023 (1)
O_1	0.5321 (2)	−0.1039 (4)	−0.0672 (3)	0.0234 (7)
O_2	0.4614 (2)	0.2626 (4)	−0.0687 (3)	0.0278 (7)
O_3	0.3648 (2)	−0.1039 (4)	−0.0672 (3)	0.0234 (7)
O_4	1.0166 (2)	1.2369 (4)	0.6011 (2)	0.0227 (7)
O_5	1.1351 (2)	0.9137 (4)	0.5873 (3)	0.0214 (7)
O_6	0.9474 (2)	0.8598 (4)	0.6161 (3)	0.0221 (7)
O_7	0.7912 (2)	0.4489 (4)	0.1633 (3)	0.0251 (7)
O_8	0.6644 (2)	0.3726 (4)	0.2639 (2)	0.0219 (7)
O_9	0.7160 (2)	0.7210 (4)	0.2492 (2)	0.0239 (7)
O_{10}	0.8311 (2)	0.4901 (3)	0.3837 (3)	0.0233 (7)
H_1	0.5646	0.0046	−0.1817	0.050
H_2	0.5935	0.7636	0.1398	0.050
H_3	0.3739	−0.1985	−0.1328	0.050
H_4	1.0776	1.3133	0.5979	0.050
H_5	1.1368	0.7691	0.5968	0.050
H_6	0.8959	0.9395	0.6439	0.050
H_7	0.7030	0.4487	−0.0169	0.050
H_8	0.6362	0.6438	−0.0631	0.050
H_9	0.6545	0.3764	−0.1350	0.050
H_{10}	0.5649	0.5574	−0.1171	0.050
H_{11}	0.8560	0.4698	0.7405	0.050
H_{12}	0.8537	0.4921	0.5675	0.050
H_{13}	0.8978	0.3546	0.6410	0.050
H_{14}	0.7840	0.4973	0.6051	0.050

$U_{eq} = 1/3 \sum_i \sum_j U_{ij} a_i * a_j * a_i a_j$.

Table 3
Thermal displacement parameters of $Cs_{0.86}(NH_4)_{1.14}SO_4Te(OH)_6$

Atoms	U_{11}	U_{22}	U_{33}	U_{23}	U_{13}	U_{12}
Te_1	0.0115(3)	0.0124(4)	0.0127(4)	−0.0005(3)	0.0036(2)	−0.0006(1)
Te_2	0.0122(3)	0.0119(4)	0.0119(4)	0.00006(1)	0.0044(2)	0.0001(1)
S	0.0121(8)	0.0134(8)	0.0156(6)	−0.0001(3)	0.0049(5)	−0.0008(3)
Cs_1	0.033(2)	0.022 (1)	0.033 (2)	−0.0022(8)	0.0111(1)	0.0042(8)
N_1	0.033(2)	0.022(1)	0.033(2)	0.0022(8)	0.0111(1)	0.0042(8)
Cs_2	0.026(2)	0.021(2)	0.025(3)	−0.0002 (1)	0.010(2)	0.0020(1)
N_2	0.026(2)	0.021(2)	0.025(3)	−0.0002 (1)	0.010(2)	0.0020(5)
O_1	0.037(2)	0.033(2)	0.029(2)	−0.013(1)	0.0225(9)	−0.0146(9)
O_2	0.0282(2)	0.0172(1)	0.032(2)	0.0027(9)	0.0000(1)	−0.0025(1)
O_3	0.0183(1)	0.0228(2)	0.030(2)	−0.0028(1)	0.0085(1)	−0.0042(9)
O_4	0.0223(2)	0.0191(1)	0.0271(2)	−0.0062(1)	0.0078(1)	0.0002(1)
O_5	0.0185(1)	0.0198(2)	0.0231(2)	−0.0027(1)	0.0013(1)	0.0003(9)
O_6	0.0260(2)	0.020 (1)	0.0239(2)	0.0060(1)	0.0146(9)	0.0010(9)
O_7	0.0258(9)	0.0295(1)	0.0230(2)	−0.0055(2)	0.0119(9)	−0.0041(9)
O_8	0.0228(9)	0.0214(9)	0.0228(2)	−0.0027(1)	0.0086(9)	−0.0044(1)
O_9	0.0250(8)	0.0144(9)	0.0309(2)	0.0008(1)	0.0060(1)	0.0015(1)
O_{10}	0.0237(2)	0.0207(2)	0.020(2)	0.0023(1)	−0.0026(1)	−0.0030(1)

The anisotropic displacement exponent takes the form: $(-2\pi^2 \sum_i \sum_j U_{ij} h_i h_j a_i a_j *)$.

Table 4
Atomic distances (Å) and angles (deg) of $Cs_{0.86}(NH_4)_{1.14}SO_4Te(OH)_6$

Distance (Å)	Distance (Å)
(a) *Cesium and ammonium coordination*	
Cs_1/N_1 Cs_2/N_2	
O_9 *c*…2.932 (4)	O_3 *k*…2.941 (6)
O_8 *d*…2.988 (4)	O_5 *l*…2.960 (6)
O_5 *e*…3.035 (4)	O_4 *m*…2.948 (4)
O_7…3.040 (5)	O_{10} …2.976 (6)
O_2 *f*…3.093 (5)	O_7 *n*…3.015 (4)
O_1 *g*…3.105 (4)	O_9 *q* …3.124 (5)
O_3 *a*…3.201 (4)	O_4 *l* … 3.296 (5)
O_1 *h*…3.312 (5)	O_6 *l*…3.295 (5)
O_2…3.037 (5)	O_6…2.856 (5)
(b) *Sulphate groups*	
S–O_7 = 1.466 (3)	O_7–S–O_9 = 109.0 (2)
S–O_9 = 1.476 (3)	O_7–S–O_{10} = 110.4 (2)
S–O_{10} = 1.482 (3)	O_9–S–O_{10} = 108.4 (1)
S–O_8 = 1.485 (3)	O_7–S–O_8 = 108.1 (2)
	O_9–S–O_8 = 110.1 (2)
	O_{10}–S–O_8 = 109.6 (2)
(c) *Tellurate groups*	
Te_1–O_3 = 1.914 (3)	O_3–Te_1–O_2 = 92.31 (11)
Te_1 _ O_3 *a* = 1.914 (3)	O_3 *a*–Te_1–O_2 = 87.69 (11)
Te_1–O_2 = 1.914 (3)	O_3–Te_1–O_1 = 88.77 (12)
Te_1–O_2 *a* = 1.914 (3)	O_3 *a*–Te_1–O_1 = 91.23 (12)
Te_1–O_1 = 1.914 (3)	O_2–Te_1–O_1 = 92.16 (13)
Te_1–O_1 *a* = 1.914 (3)	O_2 *a*–Te_1–O_1 = 87.84 (13)
Te_2–O_6 = 1.913 (3)	O_6–Te_2–O_4 *b* = 90.82 (11)
Te_2–O_6 *b* = 1.913 (3)	O_6 b–Te_2–O_4 *b* = 89.18 (11)
Te_2–O_4 = 1.916 (3)	O_6–Te_2–O_5 *b* = 90.18 (12)
Te_2–O_4 *b* = 1.916 (3)	O_6–Te_2–O_5 = 89.82 (12)
Te_2–O_5 = 1.917 (3)	O_4 *b*–Te_2–O_5 = 89.92 (11)
Te_2–O_5 b = 1.917 (3)	O_4–Te_2–O_5 = 90.08 (11)

1.907 Å and they are between 1.874(3) and 1.944(3) Å in $(NH_4)_2SO_4 \cdot Te(OH)_6$ material. The SO_4 groups are regular as seem in Table 4. The S–O distances in the tetrahedral groups are between 1.466(3) and 1.485(3) Å and the average of O–S–O angles is 109°.

In difference to the cesium and ammonium sulphate tellurate structures where the two cations do not have the same number of coordination, in the new mixed solution $Cs_{0.86}(NH_4)_{1.14}SO_4 \cdot Te(OH)_6$, the Cs/N atoms are distributed on two sites and they are nine coordinated. The (Cs/N)–O bonds ranging from 2.932(4) to 3.312(5)Å for Cs_1/N_1 and from 2.856(5) to 3.296(5)Å for Cs_2/N_2. In consequence, the distances Cs/N–O in the mixed compound $Cs_{0.86}(NH_4)_{1.14}SO_4 \cdot Te(OH)_6$ vary from 2.856(5) to 3.296(5)Å, with an average of 3.08 Å. Indeed, the environment of Cs_1/N_1 atoms is made from three oxygen atoms belonging to SO_4 groups, three to the first type of octahedra ($Te(1)O_6$), two oxygen atoms to another $Te(1)O_6$ octahedra and only one oxygen from the second octahedra $Te(2)O_6$. The Cs_2/N_2 atoms are coordinated by three oxygen atoms belonging to the SO_4 tetrahedra, one oxygen to $Te(1)O_6$ octahedra, three oxygens

Table 5
Distances and hydrogen bond angles in $Cs_{0.86}(NH_4)_{1.14}SO_4Te(OH)_6$

O…O and N…O distances (Å)	O…H distances (Å)	O…H–O and O…N–H angles (deg)
* O–H…O bonds:		
$O_4…O_{10}$ $b = 2.722$ (3)	O_{10} $b…H_4 = 1.772$ (3)	O_{10} $b…H_4–O_4 = 161.44$ (4)
$O_5…O_{10}$ $q = 2.713$ (4)	O_{10} q ….$H_5 = 1.763$ (4)	O_{10} $q…H_5–O_5 = 167.25$ (3)
$O_3…O_8$ $a = 2.787$ (4)	O_8 a …$H_3 = 1.833$ (3)	O_8 $a…H_3–O_3 = 157.24$ (2)
$O_6…O_7$ $p = 2.661$ (2)	O_7 $p…H_6 = 1.679$ (4)	O_7 $p….H_6–O_6 = 166.62$ (3)
$O_1…O_8$ $d = 2.742$ (4)	O_8 $d…H_1 = 1.845$ (3)	O_8 d …$H_1–O_1 = 160.77$ (3)
$O_2…O_9$ $f = 2.702$ (4)	O_9 $f…H_2 = 1.803$ (2)	O_9 f …$H_2–O_2 = 154.30$ (2)
* N–H…O bonds:		
$N_2…O_5$ $l = 2.960$ (4)	O_5 $l…H_{11} = 1.961$ (3)	$N_2–H_{11}…O_5$ $l = 174.61$ (1)
$N_2…O_7$ $n = 3.039$ (4)	O_7 $n…H_{12} = 2.103$ (3)	$N_2–H_{12}…O_7$ $n = 136.70$ (1)
$N_2…O_3$ $k = 2.941$ (3)	O_3 $k…H_{14} = 2.068$ (3)	$N_2–H_{14}…O_3$ $k = 149.38$ (1)
$N_2…O_4$ $m = 2.948$ (4)	O_4 $m…H_{13} = 1.969$ (4)	$N_2–H_{13}…O_4$ $m = 149.52$ (1)
$N_1…O_9 = 3.126$ (3)	O_9 $c…H_9 = 2.022$ (4)	$N_1–H_7…O_9$ $c = 151.65$ (2)
$N_1…O_7 = 3.040$ (3)	O_7 …$H_7 = 2.057$ (3)	$N_1–H_7$ …$O_7 = 156.36$ (1)
$N_1…O_1 = 3.105$ (3)	O_1 …$H_8 = 2.192$ (4)	$N_1–H_8…O_1 = 134.35$ (1)
$N_1…O_2$ $f = 3.093$ (3)	O_2 f …$H_8 = 2.256$ (4)	$N_1–H_8…O_2$ $f = 126.46$ (1)

Symmetry code: $a: -x+1, -y, -z$ $b: -x+2, -y+2, -z+1$ $c: x, -y+3/2, z-1/2$ $d: x, -y+1/2, z-1/2$ $e: -x+2, y-1/2, z-1/2$ $f: -x+1, -y+1, -z$ $g: x, y+1, z$; $h: -x+1, y+1/2, -z-1/2$ $k: -x+1, y+1/2, -z+1/2$ $l: -x+2, y-1/2, -z+3/2$ $m: x, y-1, z$ $n: -y+1/2, z+1/2$ $p: x, -y+3/2, z+1/2$ $q: -x+2, -y+1, -z+1$.

belonging to the $Te(2)O_6$ groups and two oxygen atoms to a second $Te(2)O_6$ octahedral group.

In CsNST structure, the sulphate tetrahedra are connected with tellurate octahedra by two types of hydrogen bonds O–H…O and N–H…O assured, respectively, by protons belonging to hydroxide and ammonium groups. Differently from the based compound $Cs_2SO_4 \cdot Te(OH)_6$ where only two hydrogen bonds O–H…O are detected, all the oxygen atoms belonging to SO_4 groups participate in the establishment of the first type of hydrogen bonds in the mixed compound (CsNST). In consequence, all hydrogen atoms belonging to $Te(OH)_6$ groups participate in the formation of hydrogen bonding. In sulphate group, two oxygen atoms are tied to one hydrogen atom but each other oxygen atoms are tied to two hydrogen atoms. The O…O distances are between 2.661(2) and 2.787(4) Å and the O–H…O angles vary from 154.30(2)° to 167.25(3)°. In addition to O–H…O hydrogen bonds, the structure of this mixed compound is stabilized by N–H…O hydrogen bonding. Hydrogen atoms belonging to the first and the second type of NH_4^+ group participate in the formation of this kind of hydrogen bonds. Fig. 2 shows the projection of the structure on the *ac* plane including the two types of hydrogen bonds. The presence of the two types of bonds in this structure is in the origin of the protonic conduction phase transition.

3.2. Calorimetric study

The results of the calorimetric study of the mixed cesium ammonium sulphate tellurate in the range temperature between 300 and 750 K are showed in Fig. 3.

Two endothermic peaks are observed at 470 and 500 K. By comparison with $Cs_2SO_4Te(OH)_6$, we note that the transition corresponding to paraelectric–ferroelectric phase transition at 490 K for $Cs_2SO_4Te(OH)_6$ is retained in our new mixed solution CsNST at 470 K. The endothermic peak at 500 K is attributed to the protonic conduction phase transition due to the breaking of O–H…O and N–H…O hydrogen bonds which link TeO_6 and/or NH_4 to SO_4 such that the proton moves between the potential wells associated with the anionic and cationic entities. One anomaly observed in the DSC curve about 550 K can be due to the decomposition of the salt before the melting point.

3.3. Electrical properties

Pellets, 13 mm in diameter and 1 mm in thickness, were sintered at 200-MPa pressure for 12 h under vacuum to eliminate the water content in the sample and obtain a dense pellet. Complex impedance spectra Z'' versus Z' $[-Z'' = f(Z')]$ Cole–Cole plots recorded at various temperatures are presented in Fig. 4 [17]. The complex impedance plane data show a non-depressed semi-circle for all frequency and temperature variations. The comportment of these curves shows the conductor character of our material. The resistance is determined by extrapolation at frequency equal to zero from the Z'' versus Z' circle arc centred under the Z'-axis [18].

The temperature dependence of the conductivity is presented in Fig. 5 in a log (σT) versus $1/T$ plot. We note essentially the presence of two regions. The first

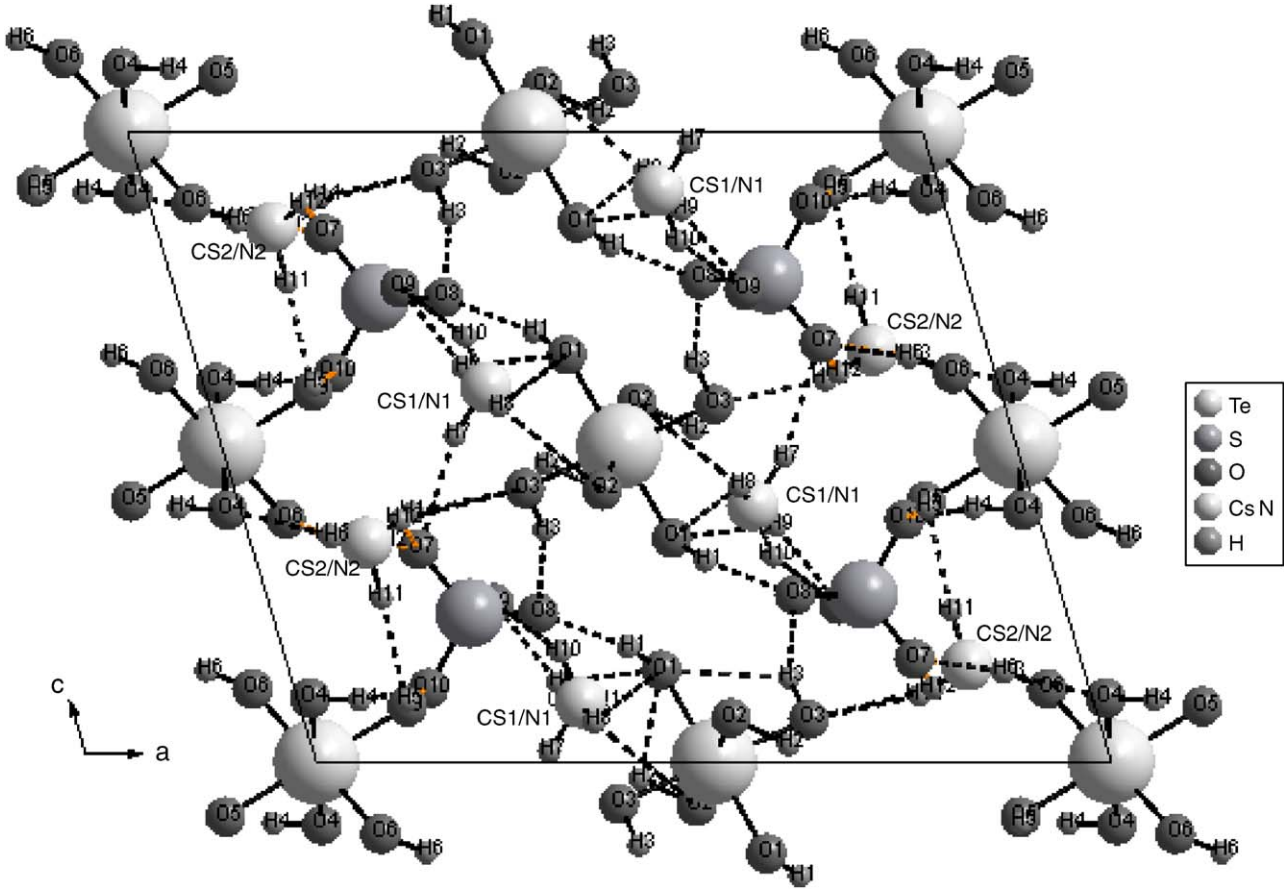

Fig. 2. Projection of the CsNST structure showing the Hydrogen bonds.

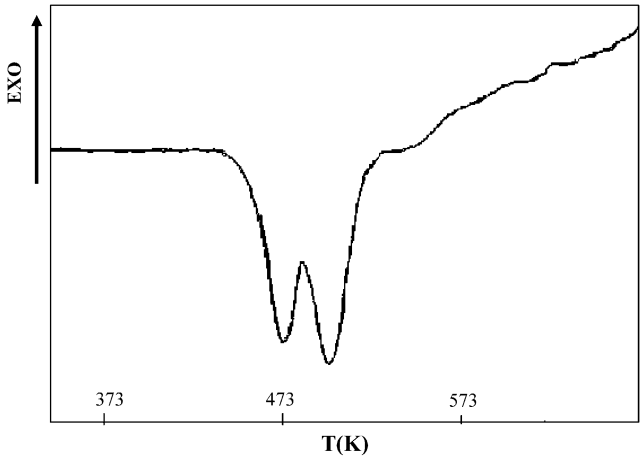

Fig. 3. Differential scanning calorimetry of $Cs_{0.86}(NH_4)_{1.14}SO_4Te(OH)_6$.

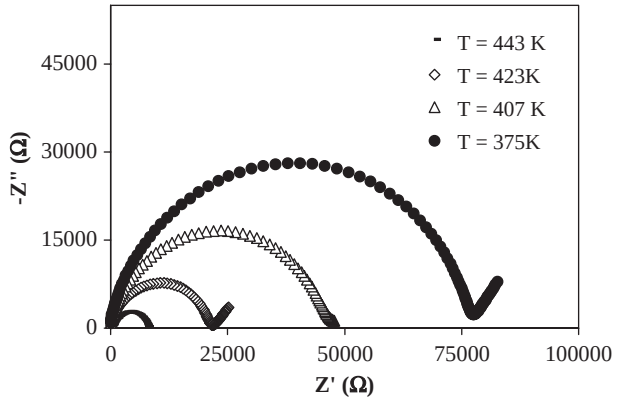

Fig. 4. Complex impedance curves of $Cs_{0.86}(NH_4)_{1.14}SO_4Te(OH)_6$ at various temperatures.

one below 500 K characterizing the conductivity at low temperature. The second one between 500 and 550 K, where we observed an abrupt rise in the electric conductivity, characterizing the superprotonic conductivity phase transition. The conductivity in these two regions obeys Arrhenius type behaviour. The high level of the conductivity at high temperatures in $Cs_{0.86}(NH_4)_{1.14}SO_4 \cdot Te(OH)_6$ can be attributed to the rapid motion of the proton H^+ due to the breaking of the hydrogen bonds. In consequence the proton H^+ becomes free between the potential holes SO_4^{2-} and TeO_6^{6-}; thus the superionic phase transition corresponds to the melting of the proton sublattice reaching the 'quasi-liquid' state where H^+, SO_4^{2-} and TeO_6^{6-} ions

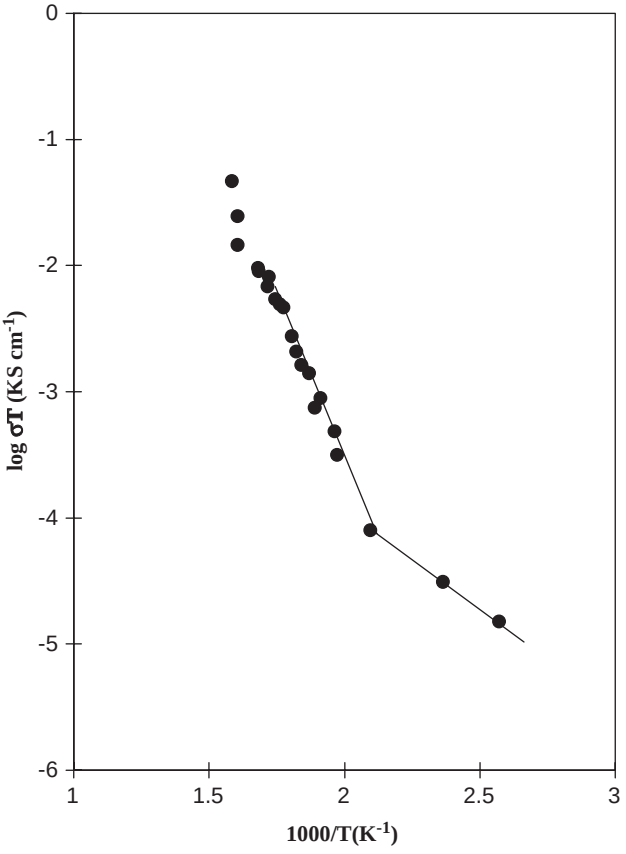

Fig. 5. Temperature dependence of $\log \sigma T$ for $Cs_{0.86}(NH_4)_{1.14}SO_4Te(OH)_6$.

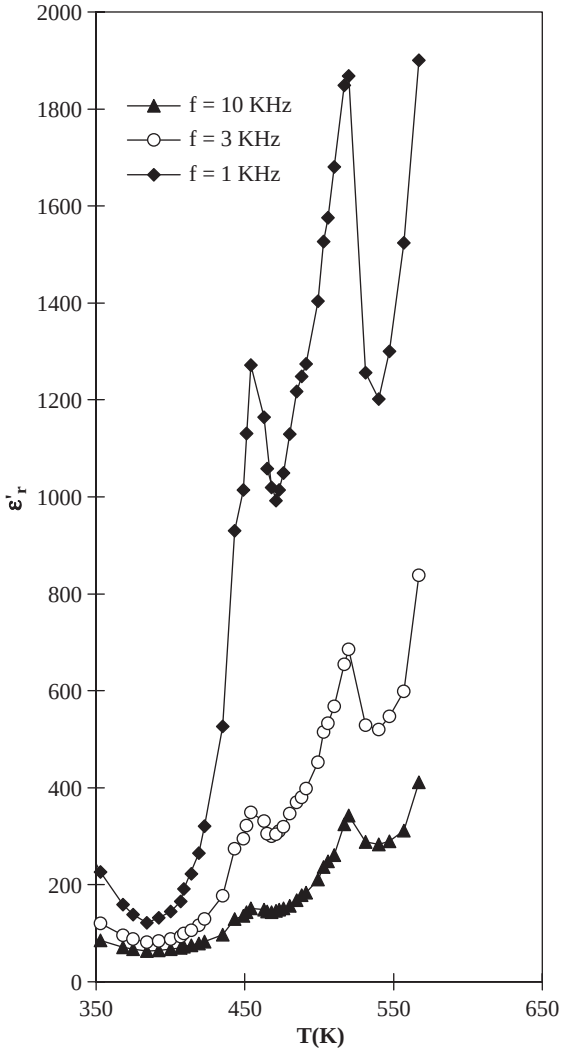

Fig. 6. Temperature dependence of ε'_r as a function of frequency for $Cs_{0.86}(NH_4)_{1.14}SO_4Te(OH)_6$.

contribute to the unusually high conductivity. At high temperatures above 550 K, the conductivity does not obey to the Arrhenius law. This behaviour is due to superposition of many mechanisms such as the protonic conduction and the decomposition of the salt before the melting point due to the dehydration of the $Te(OH)_6$ groups [1,7].

The evolution of ε'_r with the temperature is given in Fig. 6 for different frequencies. According to this figure, it is interesting to note that two anomalies on the variation of ε'_r are observed at 470 and 510 K. The second anomaly masks the decreasing of the first one. Their temperatures coincide with those observed by DSC. Temperatures of phase transition does not vary when the frequency increases, this result suggests that the compound $Cs_{0.86}(NH_4)_{1.14}SO_4 \cdot Te(OH)_6$ does not present a dielectric relaxation effect in the domain of frequencies studied. In fact, the permittivity ε'_r can be considered as the sum of two contribution [19–21]. The first contribution presents the lattice response due to permanent dipole orientation, and its anomaly characterizes the ferroelectric–paraelectric phase transition [19]. The second is manifested at low frequency, and associated to the conductivity relaxation carrier response.

The dissipation factor (tan δ) evolution as a function of temperature is presented in Fig. 7. The values are greater in agreement with the important contribution of conductivity in this material. The dielectric loss increases with increasing temperature, presents a maximum below T_c (Curie temperature) then decreases and presents a minimum in the vicinity of the transition temperature. The position of tan δ maximum depends on the frequency: it shifts to high temperature when the frequency increases. The behaviour of dielectric constant ε'_r and tan δ support the hypothesis that at 470 K the phase transition is of paraelectric–ferroelectric type as in the case of $Cs_2SO_4Te(OH)_6$ at 490 K [9].

In order to throw some additional light on the role of Cs^+ and NH_4^+ ions on the first transition, dielectric relaxation studies have consequently been undertaken in the complex modulus M^* formalism. For a given temperature and frequency, the real part M' and the imaginary part M'' of the M^* complex modulus

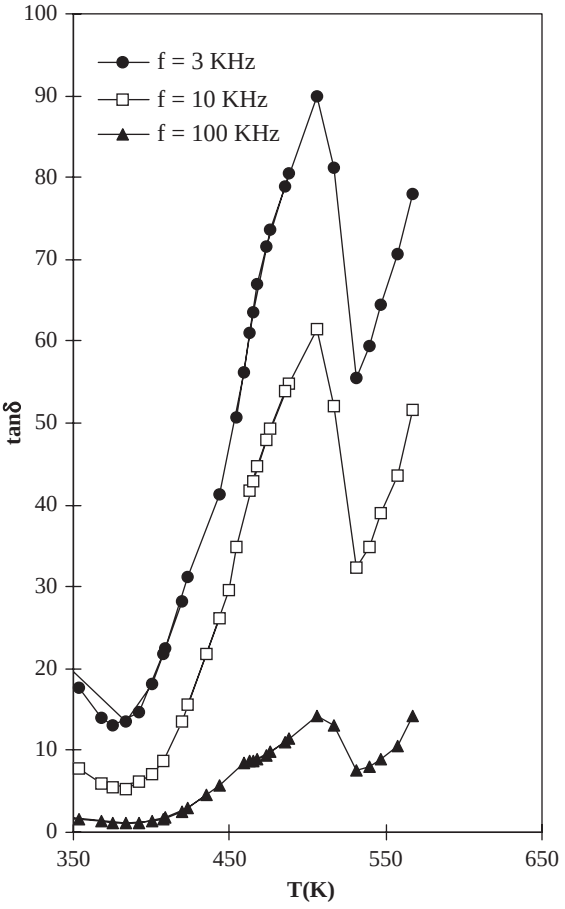

Fig. 7. Thermal evolution of the dissipation factor as a function of frequency for $Cs_{0.86}(NH_4)_{1.14}SO_4Te(OH)_6$.

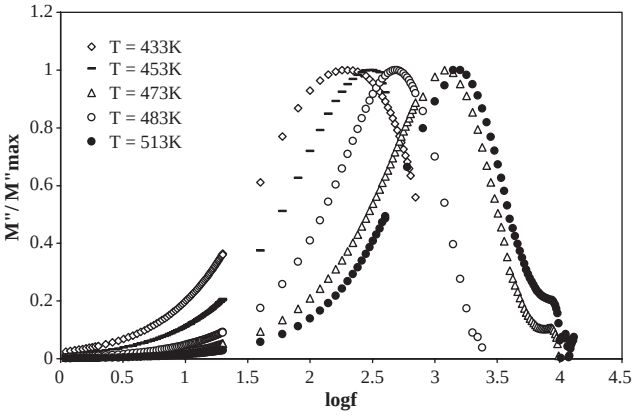

Fig. 8. Plots of log M′ versus log(*f*) for $Cs_{0.86}(NH_4)_{1.14}SO_4Te(OH)_6$ at various temperatures.

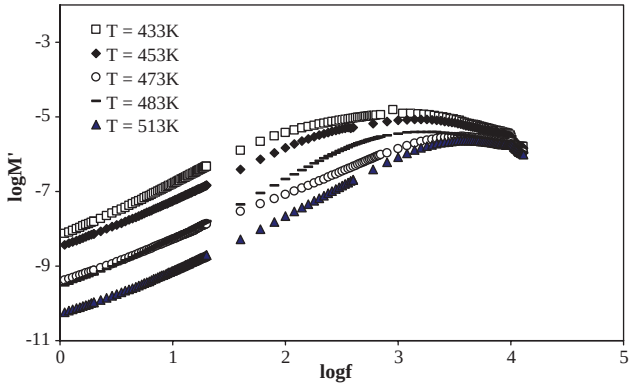

Fig. 9. Plots of normalized modulus (M''/M''_{max}) versus log(*f*) for $Cs_{0.86}(NH_4)_{1.14}SO_4Te(OH)_6$.

($M* = M' + jM''$) were calculated from the complex impedance data ($Z* = Z' - jZ''$) using the relations $M' = \omega C_0 Z''$ and $M'' = \omega C_0 Z'$. The plots of the normalized M''/M''_{max} imaginary part and $\log M'$ of the complex modulus of CsNST versus log(*f*) are given in Figs. 8 and 9 at various temperatures, respectively.

The M''/M''_{max} spectra relative to a given temperature show an asymmetrical peak characterizing the relaxation frequency of protons. From the plots of the normalized imaginary part (M''/M''_{max}), we observe that the modulus peak maximum centered in the dispersion region shifts to higher frequencies as temperatures increase.

The region of the left of the M''/M''_{max} peak maximum is where the H^+ and Cs^+/NH_4^+ ions are mobile over long distances, whereas the region of the right is where the ions are spatially confined to their potential wells. The frequency range where the peak occurs is indicative of the transition from short-range to long-range mobility at decreasing frequency and is defined by the condition $\omega\tau_\sigma = 1$, where τ_σ is the most probable constitution proton relaxation time [22]. This phenomenon is observed in $Rb_{1.12}(NH_4)_{0.88}SO_4 \cdot Te(OH)_6$ which confirms that the proton transport in $Cs_{0.86}(NH_4)_{1.14}SO_4 \cdot Te(OH)_6$ is probably due to a hopping mechanism [23,24]. From Fig. 9 (log M'), whatever the temperature, M' reaches a constant value ($M'_\infty = 1/\varepsilon_\infty$) at high frequencies and at low frequencies it approaches zero, which indicates that the electrode polarization phenomenon makes a negligible contribution to $M*$ and may be ignored when the electric data are analysed in this form [25].

4. Conclusion

The new solid solution $Cs_{0.86}(NH_4)_{1.14}SO_4 \cdot Te(OH)_6$ crystallizes in the monoclinic space group $P2_1/c$ with four formula units in the unit cell. The structure is built by TeO_6^{6-} and SO_4^{2-} anions and Cs^+/NH_4^+ cations. The main feature of the type of the mixed solution and the alcalin sulphate tellurate structures is the presence of two different and independent anions SO_4^{2-} and TeO_6^{6-} in the same unit cell which can be in the origin of important physical properties, as the ferroelectricity and the superprotonic conduction. The CsNST mixed

solution exhibits two phase transitions detected by both calorimetric and dielectric measurements.

The evolution of dielectric constant versus temperature and the conductivity versus inverse temperature for the new mixed solution $Cs_{0.86}(NH_4)_{1.14}SO_4 \cdot Te(OH)_6$ show that this material presents a paraelectric–ferroelectric phase transition at 470 K and superprotonic phase transition one manifested by a strong jump in the conductivity plot at 500 K. This ionic conductivity is attributed to H^+ and NH_4^+ mobility due to the breaking of hydrogen bonds. A relaxation study shows the H^+ transfer is probably provided by a hopping mechanism.

Acknowledgment

We wish to express our thanks to professor. M. Nierlich for his X-ray measurements and fruitful discussions and interpretations.

References

[1] M. Dammak, H. Khemakhem, N. Zouari, T. Mhiri, A.W. Kolsi, Solid State Ionics 127 (2000) 125.
[2] Z. Czapla, G. Pykach, Bull. Acad. Sci. USSR Phys. Ser. (USA) 55 (1991) 22;
Z. Czapla, G. Pykach, Transformation of I_{2v} Akad. Nank SSSR ser. Fiz. (USSR) 55 (1991) 439.
[3] S. Guillot Gauthier, J.C. Peuzin, M. Olivier, G. Rolland, Ferroelectrics 52 (1984) 293.
[4] H. Khemakhem, Ferroelectrics 234 (1999) 47.
[5] L. Ktari, M. Dammak, T. Mhiri, A.W. Kolsi, Phys. Chem. News 8 (2002) 01.
[6] L. Ktari, M. Dammak, T. Mhiri, J.M. Savariault, J. Solid State Chem. 161 (2001) 1.
[7] L. Ktari, M. Dammak, A. Hadrich, A. Cousson, M. Nierlich, F. Romain, T. Mhiri, Solid State Sci. 6 (2004) 1393.
[8] M. Dammak, T. Mhiri, J. Jaud, J.M. Savariault, J. Inorganic Mater. 3 (2001) 861.
[9] M. Dammak, H. Khemakhem, T. Mhiri, J. Phys. Chem. Solids 62 (2001) 2069.
[10] R. Zilber, A. Durif, M.T. Averbuch-Pouchot, Acta Crystallogr. B 37 (1981) 650.
[11] Nonius, Kappa CCD Server Software, Nonius B. V. Delft, The Netherlands, 1997.
[12] R. Hooft, 'Collect' Data Collection Software, Nonius B.V, The Netherlands, 1998.
[13] Z. Otwinowski, W. Minor, Methods in Enzymology, in: C.W. Carter, R.M. Sweet (Eds.), Macromolecular Crystallography. Part A, vol. 276, Academic Press, London, 1997, pp. 307–326.
[14] A.C.T. North, D.C. Philips, F.S. Mattews, Acta Crystallogr. A 39 (1968) 351.
[15] G.M. Sheldrick, SHELXS 86, program for the solution of crystal structures, Univ. of Göttingen, Germany, 1990.
[16] G.M. Sheldrick, SHELXL 93, program for crystal structure determination Univ. of Göttingen, Germany, 1993.
[17] K.S. Cole, R.H. Cole, J. Chem. Phys. 43 (1941) 341.
[18] J.F. Bauerle, J. Phys. Chem. 30 (1969) 2657.
[19] H. Khemakhem, J. Ravez, A. Daoud, Ferroelectrics 188 (1996) 41.
[20] H. Khemakhem, J. Ravez, A. Daoud, Phys. Stat. Sol. (a) 161 (1997) 557.
[21] H. Khemakhem, R. Von der Mühll, A. Daoud, J. Ravez, Phys. Stat. Sol. (a) 160 (1997) 243.
[22] H.K. Palet, S.W. Martin, Phys. Rev. B 45 (1992) 10292.
[23] L. Ktari, M. Dammak, A. Madani, T. Mhiri, A.W. Kolsi, Solid State Ionics 145 (2001) 225.
[24] B.V.R. Chowdari, R. Gopalakrishnan, Solid State Ionics 23 (1987) 225.
[25] F.S. Howell, R.A. Bose, P.B. Macedo, C.T. Moynihan, J. Phys. Chem. 78 (1974) 639.